Hindawi
Mobile Information Systems
Volume 2017, Article ID 5040347, 10 pages
https://doi.org/10.1155/2017/5040347

Research Article

Strategic Control of 60 GHz Millimeter-Wave High-Speed Wireless Links for Distributed Virtual Reality Platforms

Joongheon Kim,[1] Jae-Jin Lee,[2] and Woojoo Lee[3]

[1]*School of Computer Science and Engineering, Chung-Ang University, Seoul, Republic of Korea*
[2]*SoC Design Group, Electronics and Telecommunications Research Institute (ETRI), Daejeon, Republic of Korea*
[3]*Department of Electronics Engineering, Myongji University, Yongin, Republic of Korea*

Correspondence should be addressed to Woojoo Lee; space@etri.re.kr

Received 25 November 2016; Accepted 5 March 2017; Published 28 March 2017

Academic Editor: Konstantinos Demestichas

This paper discusses the stochastic and strategic control of 60 GHz millimeter-wave (mmWave) wireless transmission for distributed and mobile virtual reality (VR) applications. In VR scenarios, establishing wireless connection between VR data-center (called *VR server (VRS)*) and head-mounted VR device (called *VRD*) allows various mobile services. Consequently, utilizing wireless technologies is obviously beneficial in VR applications. In order to transmit massive VR data, the 60 GHz mmWave wireless technology is considered in this research. However, transmitting the maximum amount of data introduces maximum power consumption in transceivers. Therefore, this paper proposes a dynamic/adaptive algorithm that can control the power allocation in the 60 GHz mmWave transceivers. The proposed algorithm dynamically controls the power allocation in order to achieve time-average energy-efficiency for VR data transmission over 60 GHz mmWave channels while preserving queue stabilization. The simulation results show that the proposed algorithm presents desired performance.

1. Introduction

As actively discussed nowadays, virtual reality (VR) or augmented reality (AR) applications have received a lot of attention by industry and academia research organizations [1–4]. In order to provide mobile services in head-mounted VR displays in VR applications, establishing wireless connections between VR video storage (called VR server (VRS)) and head-mounted VR devices (VRD) is essential. The candidate wireless technologies should provide ultra-high-speed data communication speeds for transmitting VR video streaming without latencies.

For massive high-volume and high-definition multimedia contents delivery, millimeter-wave (mmWave) wireless communication technologies are widely discussed nowadays [5–7]. In mmWave wireless communication research, 60 GHz wireless technologies are generally and widely considered [8–11] because it is only one standardized millimeter-wave wireless technology so called IEEE 802.11ad [12].

In this paper, the 60 GHz wireless channel is explored for simultaneous large-scale massive multimedia information delivery based on following reasons:

(i) *Multigigabit-per-Second (Multi-Gbps) Data Speed*. The currently existing mmWave wireless schemes are able to support multi-Gbps data transmission speeds owing to their ultrawideband channel bandwidth. For truly immersive VR experiences, VR systems should support the high-speed data communications, which can be realized by the mmWave technologies.

(ii) *High Directionality*. mmWave wireless transmission is extremely high directional due to its high carrier frequencies. According to the fact that large-scale and densely deployed VR users will perform wireless communications, relatively high interference occurrence is expected. If the transmission beams are quite narrow, the interference impacts will be obviously reduced. Therefore, the high directionality of

mmWave propagation is beneficial in terms of the interference reduction.

Based on the 60 GHz wireless communication technologies, this paper proposes a strategic and stochastic queue control algorithm to minimize the time-average expected power consumption (which is equivalent to maximizing the time-average expected energy-efficiency) subject to queue stabilization. The VRS calculates the amount of transmit power allocation for transmitting data (from the transmission queue in VRS) to its associated VRD. If the amount of transmit power allocation at VRS is quite high, more bits will be processed from the queue within the VRS. Then, the queue should be more stable whereas power (or energy) management is not efficient. On the other hand, if the amount of transmit power allocation is relatively small, the small number of bits will be processed from the transmission queue within the VRS. Processing insufficient number of bits results in queue overflows in the VRS queue, which is not allowed because it will lose VR information at the VRS. The VR information loss should induce users' unsatisfactory experiences. Therefore, an energy-efficient stochastic transmit power allocation algorithm is required to transmit bits with the concept of the joint optimization of *energy-efficiency* and *buffer stability*.

The last sections of this paper are as follows: the reference distributed VR network platforms is introduced in Section 2. The next section introduces 60 GHz wireless technologies with 60 GHz IEEE 802.11ad standards. Based on the introduction, the methodologies for estimating maximum communication speeds are presented in Section 3. In Section 4, strategic and stochastic control for mmWave transmit powers for the minimization of time-average expected power consumption subject to queue stabilization is proposed based on 60 GHz mmWave wireless channel understanding. The related intensive simulation results are presented in Section 5, while Section 6 concludes this paper.

2. Reference Mobile Virtual Reality Network Model with 60 GHz Millimeter-Wave Wireless Links

Current VRDs support 360-degree video applications to allow users to interact with digital environments and objects. For example, according to users' head motions such as pitching (leaning forward/backward), yawing (rotating left/right), and rolling (spinning clockwise/counterclockwise), the state-of-the-art VRDs offer corresponding video images to the users. Oculus GearVR [13] is a representative one of such VRDs in market, which nicely provides 4K full HD video playback.

However, unfortunately, it is hard to agree that current VRDs are providing the truly immersive VR experiences that have been an aspiration of many. That is because the truly immersive VR systems should have three essential features: quality, responsiveness, and mobility [14]. The quality means the realistic visual portrayals, which should be based on high resolution video images. For instance, videos at 6K resolution (i.e., the 6K video streaming service already exists in market) or videos at 8K resolution may be the candidate to provide such high quality visual portrayals. The responsiveness means how fast a user's motion is reflected to the video playback in a VRD. Due to very high sensitivity of human ocular proprioception, immediate feedback from the motion to the VRD display is necessary, whereas the current VR systems may not be able to support such fast responsiveness. Meanwhile, the mobility is regarding a question of what we can do in real world but cannot in the current VR systems. Namely, we can move left/right, go forward/backward, and jump up/down, which may cause nothing in the current (typical) VRDs.

Extensive research efforts have been invested to overcome the limitations of the current VR systems, thereby meeting the aforesaid requirements. For example, Facebook has proposed the dynamic streaming technique to provide 6K video streaming service [15]. Furthermore, tremendous efforts on new video codecs to support high quality video with high efficiency make us expect that the high resolution videos will be no longer an issue in near future. For the fast responsiveness issue, embedding the bigger size caches (thanks to semiconductor technology progress) into VRDs seems to be a plausible solution; in that a VRD then rarely needs to send its motion information to a VRS and wait for the corresponding video data to be delivered from a VRS. For the mobility issue, researchers have recently started studying on motion parallax [16], which has been driving the advent of 8K video applications. By taking a user's position and direction into consideration, these 8K video applications are beyond the conventional three degrees of freedom (DoF) and enable any motions to be reflected.

Nevertheless, the truly immersive VR systems do still have a major challenge, the high-speed VR network. As rising resolution of video applications including various parallaxes of each single image, the video applications require a lot of data and delivery of these experiences across the Internet presents the inevitable challenge on network (i.e., even 6K resolution used by the GearVR may be 20 times the size of 4K videos). We have searched on the most possible solutions and eventually determined that the mmWave-based network is the strongest candidate for the near future VR system.

Our proposed model of the VR system including mmWave-based VR network is described in Figure 1. One or multiple mmWave antennas are deployed in the system, each of which supports the GHz data transmission. The user's requests, for example, motion changes and VRD controls, are delivered to the VRS, and the VRS performs appropriate actions such as serving different video streaming, sending different parallax images in the playing video, and compressing the video with different codec. The mux logic in the figure shows one of the control ways that the VRS carries out to respond to the corresponding user information. When the video data is delivered, each data is piled up in the buffers. The VRD may have multilayer buffers to realize various controls in the video playback.

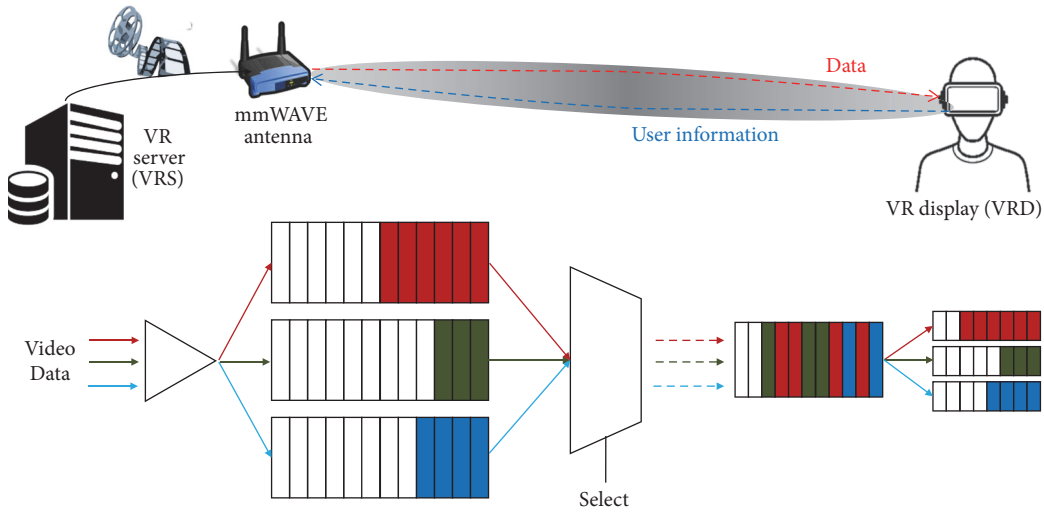

Figure 1: Concept of the proposed VR system exploiting the mmWave-based VR network.

3. Maximum Communication Speed of 60 GHz Wireless Systems with IEEE 802.11ad Standard Features

This section mathematically calculates the maximum speed (i.e., upper bound) of wireless data transmission over 60 GHz mmWave channels and eventually defines the quality of VR video streaming, through the following steps: (i) calculating the received signal strength at VRD, (ii) obtaining maximum wireless data transmission speed, and (iii) defining the quality of streaming. The maximum wireless data transmission speed will be derived with two possible ways: (i) using Shannon capacity equation and (ii) using the level of supportable modulation and coding scheme (MCS) defined in IEEE 802.11ad specification and its associated wireless data transmission speed.

3.1. Calculation of the Received Signal Strength at VRD. The received signal strength in 60 GHz mmWave wireless channels that depends on distance between VRS and VRD (denoted by d) at VRD in a milli-Watt scale, $P_{\mathrm{mW}}^{\mathrm{VRD}}(d)$, can be calculated as follows:

$$P_{\mathrm{mW}}^{\mathrm{VRD}}(d) = f_{\mathrm{mW}}\left(P_{\mathrm{dBm}}^{\mathrm{VRD}}(d)\right), \tag{1}$$

where $f_{\mathrm{mW}}(x) = 10^{x/10}$ and $P_{\mathrm{dBm}}^{\mathrm{VRD}}(d)$, that is, the received signal strength in 60 GHz mmWave wireless channels depending on distance between VRS and VRD (denoted by d) at VRD in a dB scale, can be obtained as follows:

$$P_{\mathrm{dBm}}^{\mathrm{VRD}}(d) = G_{\mathrm{dBi}}^{\mathrm{VRS}} + P_{\mathrm{dBm}}^{\mathrm{VRS}} - L(d) + G_{\mathrm{dBi}}^{\mathrm{VRD}}, \tag{2}$$

where $G_{\mathrm{dBi}}^{\mathrm{VRS}}$, $G_{\mathrm{dBi}}^{\mathrm{VRD}}$, and $P_{\mathrm{dBm}}^{\mathrm{VRS}}$ are the transmit antenna gain at VRS in a dB scale, the receive antenna gain at VRD in a dB scale, and the transmit power (assumed to be 19 dBm [17]) at VRS in a dB scale, respectively; $L(d)$ is the path-loss that depends on d. In the equation, $G_{\mathrm{dBi}}^{\mathrm{VRS}} = 24$ dBi according to [17], and we assume $G_{\mathrm{dBi}}^{\mathrm{VRD}} = 0$ dBi, which corresponds to the omnidirectional receive antenna at VRD. Note that assuming omnidirectional receive antenna at VRD is beneficial because it reduces beam training time overhead that is essential for mobile mmWave services as clearly discussed in [18].

According to the 60 GHz IEEE 802.11ad line-of-sight (LOS) path-loss [19], the dB scaled $L(d)$ in (2) can be defined as follows:

$$L(d) = A + 20\log_{10}\left(f_{\mathrm{GHz}}\right) + 10n\log_{10}(d), \tag{3}$$

where A is a specific value for the selected type of antenna and beamforming algorithm that relies on the antenna beamwidth, that is, $A = 32.5$ dB, as defined in [19]. In addition, the path-loss coefficient n is set to 2, and f_{GHz} is the carrier frequency in GHz; thereby $f_{\mathrm{GHz}} = 60$. The direct paths between VRS and VRD have no obstacles; thus LOS model is considered in this research.

Based on the calculation result of the received signal strength in VRD, the interfering signals are added to the desired transmission through the main wireless link from VRS to VRD. Therefore, signal-to-interference plus noise ratio (SINR) in a dB scale, denoted by γ_{dB}, can be obtained as follows:

$$\gamma_{\mathrm{dB}}(d) = f_{\mathrm{dB}}\left(\frac{P_{\mathrm{mW}}^{\mathrm{VRD}}(d)}{n_{\mathrm{mW}} + \sum_{i \in S_I} I_{\mathrm{mW}}^{i}}\right), \tag{4}$$

where $f_{\mathrm{dB}}(x) = 10 \cdot \log_{10}(x)$ and n_{mW} is a background noise in a milli-Watt scale that can be derived as follows [20]:

$$n_{\mathrm{mW}} = f_{\mathrm{mW}}\left(k_B T_e + 10\log_{10} B + F_n\right). \tag{5}$$

In (5), $k_B T_e$ is a noise power spectral density which is -174 dBm/Hz [20], B is one subchannel bandwidth in 60 GHz mmWave which is defined as 2.16 GHz in IEEE 802.11ad [5], and F_n is a noise figure which is assumed to be 5 dB [12]. S_I in (4) is a set of the wireless transmissions from VRS to VRD (those are not our main considering VR wireless communications) excluding the aforementioned main video

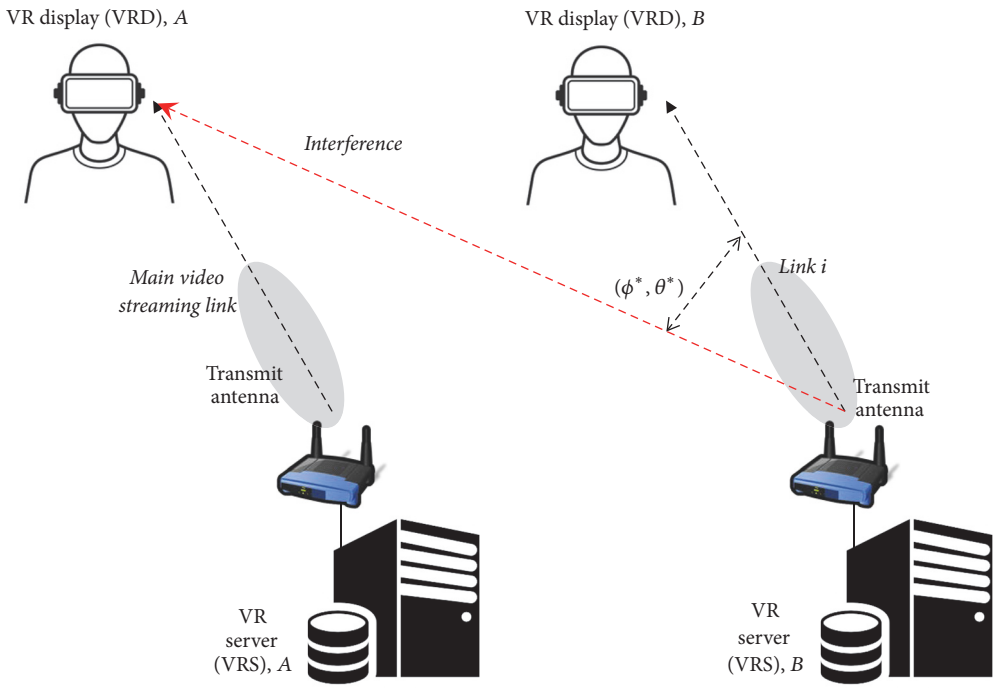

Figure 2: Interference scenario with directional transmit antennas.

streaming, that is, a set of interference transmissions. In addition, I^i_{mW} means the interference in a milli-Watt scale to our main VRD induced by the neighbor 60 GHz mmWave wireless transmissions from links i where $i \in S_I$. In a consequence, the interference from the 60 GHz mmWave wireless link i can be expressed as follows:

$$I^i_{\mathrm{mW}} = f_{\mathrm{mW}}\left(G^{i,\mathrm{VRS}}_{\mathrm{dBi}}(\theta^*, \phi^*) + P^{i,\mathrm{VRS}}_{\mathrm{dBm}} - L(d_i)\right), \quad (6)$$

where $P^{i,\mathrm{VRS}}_{\mathrm{dBm}}$ stands for the transmit power from the VRS of 60 GHz mmWave wireless link i and $L(d_i)$ is the path-loss in (3) for d_i, that is, the distance between the VRS of link i and the VRD of the main video streaming. Lastly, $G^{i,\mathrm{VRS}}_{\mathrm{dBi}}(\theta^*, \phi^*)$ is the transmit antenna radiation gain from the transmitter of 60 GHz mmWave wireless link i to the VRD of main video streaming. It means that θ^* and ϕ^* are the azimuthal and elevational angular differences between two links (one link is main video streaming and the other link is wireless link i).

Figure 2 provides an example for the interference scenario. As illustrated in Figure 2, there exist two parallel VR wireless data transmissions. One is from the VRS of main video streaming (named VRS A in Figure 2) to its associated VRD (named VRD A in Figure 2) of main video streaming; and the other one is from VRS of wireless link i (named VRS B in Figure 2) to its associated VRD of wireless link i (named VRD B in Figure 2).

θ^* and ϕ^* are the azimuth and elevation angular differences between the link i and main video streaming, respectively. As illustrated in Figure 2, the directional wireless transmission from VRS B to VRD B will be one potential interference source to the VRD A.

3.2. Obtaining Maximum Wireless Data Transmission Speed. In order to obtain the maximum wireless data transmission speed, two possible methods may exist: (i) using Shannon capacity equation (refer to Section 3.2.1) and (ii) using the level of supportable MCS defined in IEEE 802.11ad specification and its associated wireless data transmission speed (refer to Section 3.2.2).

3.2.1. Using Shannon Capacity Equation. Based on the SINR calculated in (4) in Section 3.1, the theoretical maximum wireless data transmission speed is formulated as

$$B \cdot \log_2\left(\gamma_{\mathrm{dB}}(d)\right), \quad (7)$$

where B is one subchannel bandwidth, which is 2.16 GHz in 60 GHz mmWave wireless systems.

3.2.2. Using the Level of Supportable MCS Defined in IEEE 802.11ad Specification and Its Associated Wireless Data Transmission Speed. This subsection uses $\gamma_{\mathrm{dB}}(d)$ which resulted from the previous step in Section 3.1. The derived $\gamma_{\mathrm{dB}}(d)$ will be compared with the receiver sensitivity defined in IEEE 802.11ad specification [12]. The receiver sensitivity values and their associated supportable wireless data transmission speeds are summarized in Table 1 [12]. However, the direct comparison between $r_{\mathrm{dB}}(d)$ and the values in Table 1 [12] may not be possible. Instead, the values should be converted to signal-to-noise ratio (SNR) as

$$\mathrm{SNR}^k_{\mathrm{dB}} = [\text{Receiver-Sensitivity}]^k - n_{\mathrm{dBm}}, \quad (8)$$

where $[\text{Receiver-Sensitivity}]^k$ is a receiver sensitivity of MCS level k; $\mathrm{SNR}^k_{\mathrm{dB}}$ is the associated corresponding SNR of the

Table 1: IEEE 802.11ad single-carrier MCS table [12].

Receiver Sensitivity	Selected MCS indices (Data rates, unit: Mbps)
−78 dBm	MCS0 (27.5)
−68 dBm	MCS1 (385)
−66 dBm	MCS2 (770)
−65 dBm	MCS3 (962.5)
−64 dBm	MCS4 (1155)
−63 dBm	MCS6 (1540)
−62 dBm	MCS7 (1925)
−61 dBm	MCS8 (2310)
−59 dBm	MCS9 (2502.5)
−55 dBm	MCS10 (3080)
−54 dBm	MCS11 (3850)
−53 dBm	MCS12 (4620)

receiver sensitivity of MCS level k, and n_{dBm} is a background noise in a dB scale as previously presented in (5). When the obtained $\gamma_{\mathrm{dB}}(d)$ value in Section 3.1 is in between $\mathrm{SNR}^{i}_{\mathrm{dB}}$ (i.e., the SNR of MCS index i (lower)) and $\mathrm{SNR}^{j}_{\mathrm{dB}}$ (i.e., the SNR of MCS index j (higher)), the 60 GHz mmWave wireless link of the main video streaming uses the MCS index i. Once we determine the supportable MCS level, the associated wireless data transmission speed is obtained from Table 1.

3.3. Quality Estimation of Wireless Video Streaming [12]. In order to estimate the quality of the wireless video streaming that depends on the derived maximum wireless data transmission speed, we use the model presented in [5, 12]. This section summaries the discussion in [5, 12]. The wireless transmission of 1080 p @ 30 fps (30 frames, each of which has 1080-by-1920 pixels, will be presented in a display per second) in RGB (8 bits for each Red/Green/Blue color representation, i.e., $8 \times 3 = 24$ bits) video frames with no compression (no source coding but only channel coding exists) requires the 1.5-gigabit/s (Gbps) wireless data transmission speed since each frame has 1920×1080 pixels with 30 frames per second, and each pixel has 24 bits in an RGB format. Similarly, the wireless data transmission speed of 3 Gbps is at least required for the full-quality 1080 @ 60 fps streaming in RGB (i.e., $1080 \times 1920 \times 24 \times 60$). In YCbCr 4 : 2 : 0 formats, the required wireless data transmission speed is half of the wireless data transmission speed in RGB formats; that is, 0.75 Gbps and 1.5 Gbps speeds are required for nonsource-coded real-time 1080 p @ 30 fps and 1080 p @ 60 fps video streaming, as introduced. If the maximum wireless data transmission speed calculated and obtained in Sections 3.1 and 3.2 is less than the full-quality threshold, the quality may degrade. One widely suggested reference model of the quality is as [5, 12]

$$f_q(x) = \begin{cases} \dfrac{1}{\log_\alpha(x_{\max}+1)} \log_\alpha(x+1), & \text{if } x < x_{\max}, \\ x_{\max}, & \text{otherwise}, \end{cases} \tag{9}$$

where α is a base ($1 < \alpha$), $x_{\max}$ is a desired wireless data transmission speed for the uncompressed streaming (i.e., 0.75 Gbps in 1080 @ 30 fps in YCbCr 4 : 2 : 0 formats; 1.5 Gbps in 1080 p @ 60 fps in YCbCr 4 : 2 : 0 formats; 1.5 Gbps in 1080 p @ 30 fps in RGB formats; and 3.0 Gbps in 1080 p @ 60 fps in RGB formats), and x is the achievable wireless data transmission speed derived in Sections 3.1 and 3.2.

4. Proposed Strategic Control of 60 GHz Wireless Communications in Mobile Virtual Reality Applications

4.1. Design Rationale. For each wireless transmission from VRS to VRD, if the transmission queue in VRS is almost empty, the transmission algorithm should not need to allocate a lot of transmit power in order to transmit more bits from the queue. Then, the algorithm will allocate relatively little amount of powers into the transmitter in order to work in the energy-efficient manner. On the other hand, if the transmission queue in VRS is almost occupied by VR data information (almost in the overflow situations), the transmission algorithm should allocate relatively large amount of powers into the transmitter in order to avoid the queue-overflow situations. Therefore, this section proposes a stochastic optimization framework that works for the minimization of time-average expected power consumption (which is equivalent to the maximization of time-average expected energy-efficiency), while preserving queue stabilization that depends on the queue-backlog sizes in each unit time.

4.2. Strategic Control of 60 GHz Wireless Virtual Reality Applications. For each VRS $v_i \in \mathscr{V}$ where $\mathscr{V}$ is the set of existing wireless links between VRSs and VRDs, the queue dynamics in unit time $t \in \{0, 1, \ldots\}$ can be formulated as follows:

$$\begin{aligned} Q_i[t+1] &= \left(Q_i[t] - \mu_i[t] + \lambda_i[t]\right)^+, \\ Q_i[0] &= 0, \end{aligned} \tag{10}$$

where $(a)^+ \triangleq \max\{a, 0\}$ and $Q_i[t]$, $\mu_i[t]$, and $\lambda_i[t]$ mean the queue backlog at VRS $\forall v_i \in \mathscr{V}$ at t, the departure process (i.e., wireless transmission of VR videos to VRD) from VRS $\forall v_i \in \mathscr{V}$ at t, and the arrival process (i.e., VR video chunk placement) to VRS $\forall v_i$ at t, respectively. The unit of $Q_i[t]$, $\mu_i[t]$, and $\lambda_i[t]$ is bit. Here, $\mu_i[t]$ and $\lambda_i[t]$ mean the amounts of transmitted bits from VRS $\forall v_i \in \mathscr{V}$ to its associated VRD at unit time t over 60 GHz mmWave wireless channels and the generated data in VRS $\forall v_i \in \mathscr{V}$ to be transmitted to its associated VRD at unit time t over 60 GHz mmWave wireless channels, respectively. Notice that the arrival process is independent of power allocation decision.

In order to formulate $\mu_i[t]$, we consider the case whereby the maximum wireless data transmission speed is obtained from the Shannon capacity equation. Then, according to (1) and (2), it is obvious that

$$\mu_i[t] = B \cdot \log_2\left(\gamma_{\mathrm{dB}}(d)\right) \tag{11}$$

$$= B \cdot \log_2\left(f_{\mathrm{dB}}\left(\frac{P^{\mathrm{VRD}}_{\mathrm{mW}}(d)}{n_{\mathrm{mW}} + \sum_{i \in S_I} I^{i}_{\mathrm{mW}}}\right)\right) \tag{12}$$

Parameters;
(i) V: a parameter for power-delay (queueing delay) tradeoffs
(ii) B: channel bandwidth (2.16 GHz in 60 GHz mmWave wireless systems)
(iii) n_{mW}: background noise
(iv) $G_{\mathrm{dBi}}^{\mathrm{VRS}}$: transmit antenna gain at VRS
(v) $\mathscr{P}$: a set of possible power allocation candidates
(vi) S_I: a set of possible interference sources
Stochastic Power Allocation for the Transceiver of VR Server (VRS);
$t = 0$;
// $T_{\max}$: the number of discrete-time operation;
while $t \leq T_{\max}$ **do**
(i) Observes $Q_i[t]$, d, and I_{mW}^i;
(ii) Finds stochastic optimal power allocation $P_{i,\mathrm{dBm}}^{\mathrm{VRS}}[t]$ in $\mathscr{P}$ which can minimize;

$$P_{i,\mathrm{dBm}}^{\mathrm{VRS}}[t] - VBQ_i[t]\log_2\left(f_{\mathrm{dB}}\left(\frac{f_{\mathrm{mW}}\left(G_{\mathrm{dBi}}^{\mathrm{VRS}} + P_{i,\mathrm{dBm}}^{\mathrm{VRS}}[t] - L(d)\right)}{n_{\mathrm{mW}} + \sum_{i\in S_I} I_{\mathrm{mW}}^i}\right)\right)$$

Algorithm 1: Stochastic power allocation for the minimization of time-average expected power consumption subject to queue-stabilization in the transceiver of virtual reality (VR) servers.

$$= B \cdot \log_2\left(f_{\mathrm{dB}}\left(\frac{f_{\mathrm{mW}}\left(G_{\mathrm{dBi}}^{\mathrm{VRS}} + P_{\mathrm{dBm}}^{\mathrm{VRS}} - L(d) + G_{\mathrm{dBi}}^{\mathrm{VRD}}\right)}{n_{\mathrm{mW}} + \sum_{i\in S_I} I_{\mathrm{mW}}^i}\right)\right) \quad (13)$$

$$= B \cdot \log_2\left(f_{\mathrm{dB}}\left(\frac{f_{\mathrm{mW}}\left(G_{\mathrm{dBi}}^{\mathrm{VRS}} + P_{\mathrm{dBm}}^{\mathrm{VRS}} - L(d)\right)}{n_{\mathrm{mW}} + \sum_{i\in S_I} I_{\mathrm{mW}}^i}\right)\right). \quad (14)$$

Note that $G_{\mathrm{dBi}}^{\mathrm{VRD}}$ is disappeared in (14) because $G_{\mathrm{dBi}}^{\mathrm{VRD}} = 0$ dBi (again, we supposed the omnidirectional receiver antenna setting).

The mathematical program to minimize the summation of the time-average expected power consumption (which is obviously equivalent to the maximization of the summation of time-average expected energy-efficiency) is as follows:

$$\min \quad \sum_{v_i\in\mathscr{V}} \mathbb{E}\left[P_{i,\mathrm{dBm}}^{\mathrm{VRS}}\right], \quad (15)$$

where $\mathbb{E}[P_{i,\mathrm{dBm}}^{\mathrm{VRS}}]$ stands for the time-average expected power consumption at $v_i \in \mathscr{V}$, and this is equivalent to

$$\min \quad \sum_{v_i\in\mathscr{V}} \left(\lim_{t\to\infty}\frac{1}{t}\sum_{\tau=0}^{t-1} P_{i,\mathrm{dBm}}^{\mathrm{VRS}}[\tau]\right). \quad (16)$$

Note the objective function in our stochastic optimization framework has the following two constraints: (i) a constraint for queue rate stability and (ii) a constraint for discretized power allocation due to radio frequency (RF) hardware design limitations (i.e., it is impossible to allocation real-number scaled transmit powers). The first can be expressed as

$$\lim_{t\to\infty}\frac{1}{t}\sum_{\tau=0}^{t-1}\frac{\mathbb{E}\left[Q_i[\tau]\right]}{\tau} = 0, \quad \forall v_i \in \mathscr{V}, \quad (17)$$

and we can rewrite (17) in this formulation:

$$\lim_{t\to\infty}\frac{1}{t}\sum_{\tau=0}^{t-1}\mathbb{E}\left[Q_i[\tau]\right] < \infty, \quad \forall v_i \in \mathscr{V}. \quad (18)$$

The constraint for discretized power allocation can be expressed as

$$P_{i,\mathrm{dBm}}^{\mathrm{VRS}}[t] \in \mathscr{P} \triangleq \left\{p_{\min}, p_1, p_2, \ldots, p_{\max}\right\}. \quad (19)$$

Now, let us introduce a new variable $\Theta(t)$ that denotes the column vector of all queues in VRSes at unit time t and iteratively define the quadratic Lyapunov function $L[t]$ as follows:

$$L[t] = \frac{1}{2}\Theta^T[t]\,\Theta[t] = \frac{1}{2}\sum_{v_i\in\mathscr{V}}\left(Q_i[t]\right)^2, \quad (20)$$

where $\Theta^T[t]$ denotes the transpose of $\Theta[t]$. Then, let us introduce another new variable $\Delta[t]$ that is a conditional quadratic Lyapunov function that may be formulated as follows:

$$\Delta[t] \triangleq \mathbb{E}\left[L[t+1] - L[t] \mid \Theta[t]\right], \quad (21)$$

that is, the drift on unit time t. The decision-making policy of the dynamic and stochastic power allocation is designed to (i) solve the minimization of time-average expected power consumption formulation by observing the current queue-backlog sizes $Q_i[t]$ and (ii) iteratively determine the amount of power allocation $P_{i,\mathrm{dBm}}^{\mathrm{VRS}}$ for maximizing a bound on

$$\mathbb{E}\left[P^{\mathrm{VRS}}[t] \mid \Theta[t]\right] - V\Delta[t], \quad (22)$$

where $P^{\mathrm{VRS}}[t]$ is the column vector of $P_{i,\mathrm{dBm}}^{\mathrm{VRS}}[t]$, $\forall v_i \in \mathscr{V}$, and V is the positive constant control parameter setting of the dynamic/stochastic decision-making policy that affects the power-delay (i.e., queueing delay) tradeoffs.

The proposed algorithm involves minimizing a bound on $\mathbb{E}[P^{\mathrm{VRS}}[t] \mid \Theta[t]] - V\Delta[t]$; and finally this Lyapunov optimization theory gives Algorithm 1 to minimize the following equation:

$$\sum_{v_i\in\mathscr{V}} P_{i,\mathrm{dBm}}^{\mathrm{VRS}}[t] + V\sum_{v_i\in\mathscr{V}} Q_i[t]\left(\lambda_i[t] - \mu_i[t]\right). \quad (23)$$

In (23), $\lambda_i[t]$ is independent of power allocation and thus it is not controllable by power allocation. Therefore, it can be ignored; that is,

$$\sum_{v_i \in \mathscr{V}} P_{i,\mathrm{dBm}}^{\mathrm{VRS}}[t] - V \sum_{v_i \in \mathscr{V}} Q_i[t]\,\mu_i[t]. \tag{24}$$

According to the fact that $\mu_i[t]$ can be derived by (14), finally (24) is reformulated as follows:

$$\sum_{v_i \in \mathscr{V}} P_{i,\mathrm{dBm}}^{\mathrm{VRS}}[t] - V \cdot B \cdot \sum_{v_i \in \mathscr{V}} Q_i[t] \cdot \log_2\left(f_{\mathrm{dB}}\left(\frac{f_{\mathrm{mW}}\left(G_{\mathrm{dBi}}^{\mathrm{VRS}} + P_{i,\mathrm{dBm}}^{\mathrm{VRS}}[t] - L(d)\right)}{n_{\mathrm{mW}} + \sum_{i \in S_I} I_{\mathrm{mW}}^{i}}\right)\right), \tag{25}$$

where $P_{i,\mathrm{dBm}}^{\mathrm{VRS}}[t]$ is the transmit power allocation at VRS in a dB scale at unit time t in $v_i \in \mathscr{V}$.

In (25), it is clear that the given equation (25) is separable; that is, the separated minimization of the objective function of each VRS $\forall v_i \in \mathscr{V}$ introduces the minimization of (25). Therefore, each VRS $\forall v_i \in \mathscr{V}$ minimizes its own objective function as follows:

$$P_{i,\mathrm{dBm}}^{\mathrm{VRS}}[t] - V \cdot B \cdot Q_i[t] \cdot \log_2\left(f_{\mathrm{dB}}\left(\frac{f_{\mathrm{mW}}\left(G_{\mathrm{dBi}}^{\mathrm{VRS}} + P_{i,\mathrm{dBm}}^{\mathrm{VRS}}[t] - L(d)\right)}{n_{\mathrm{mW}} + \sum_{i \in S_I} I_{\mathrm{mW}}^{i}}\right)\right). \tag{26}$$

From this given (26), we have to find the amount of power allocation that minimizes (26). Therefore, our final closed-form solution is as follows:

$$P_{i,\mathrm{dBm}}^{*,\mathrm{VRS}}[t] \longleftarrow \arg \min_{P_{i,\mathrm{dBm}}^{\mathrm{VRS}}[t] \in \mathscr{P}} \left\{P_{i,\mathrm{dBm}}^{\mathrm{VRS}}[t] - VBQ_i[t] \log_2\left(f_{\mathrm{dB}}\left(\frac{f_{\mathrm{mW}}\left(G_{\mathrm{dBi}}^{\mathrm{VRS}} + P_{i,\mathrm{dBm}}^{\mathrm{VRS}}[t] - L(d)\right)}{n_{\mathrm{mW}} + \sum_{i \in S_I} I_{\mathrm{mW}}^{i}}\right)\right)\right\}. \tag{27}$$

The entire stochastic procedure is also described in Algorithm 1.

5. Performance Evaluation

This section consists of (i) simulation parameter settings (refer to Section 5.1) and (ii) performance evaluation in terms of queue dynamics and energy-efficiency (refer to Section 5.2), respectively.

5.1. Simulation Settings. For evaluating the performance of our proposed queue-stable time-average expected power consumption minimization algorithm, the following simulation parameters are used:

(i) Transmit antenna gain: 15 dBi [17].

(ii) Transmit power allocation set $\mathscr{P}$ in (19) [17]:

$$\mathscr{P} \triangleq \{p_{\min} = 10\,\mathrm{dBm},\ p_1 = 13\,\mathrm{dBm},\ p_2 = 16\,\mathrm{dBm},\ p_{\max} = 19\,\mathrm{dBm}\} \tag{28}$$

(iii) The number of interfering sources: 3.

(iv) V settings (three different values):

$$V \triangleq \left\{V_1 = 1 \times 10^{-23},\ V_2 = 5 \times 10^{-23},\ V_3 = 5 \times 10^{-24}\right\} \tag{29}$$

For the simulation study in this paper, we have three different simulation results; those are conducted with three different V settings, that is, $V = V_1 = 1 \times 10^{-23}$ (for Figures 3(a) and 3(b)), $V = V_2 = 5 \times 10^{-23}$ (for Figures 3(c) and 3(d)), and $V = V_3 = 5 \times 10^{-24}$ (for Figures 3(e) and 3(f)).

5.2. Simulation Results. In this section, we tracked the queue dynamics and energy consumption behaviors as plotted in Figure 3. As shown in Figure 3, the proposed strategic control algorithm shows stable performance. If the queue-backlog size reaches certain levels, the proposed stochastic and strategic algorithm tries to stabilize the queue backlogs. As presented in Figures 3(a), 3(c), and 3(e), the queue-backlog sizes are stabilized near 1.5×10^{13} bits, 0.5×10^{13} bits, and 3×10^{13} bits, respectively. Comparing to the performance of the proposed algorithm with $V = V_1 = 1 \times 10^{-23}$, the performance of the proposed algorithm with $V = V_2 = 5 \times 10^{-23}$ takes more queue stability because the average queue-backlog size becomes more smaller. It means that the proposed algorithm with $V = V_2 = 5 \times 10^{-23}$ pursues more queue stabilization. In addition, the proposed algorithm with $V = V_3 = 5 \times 10^{-24}$ allows more queue-backlog sizes (i.e., allowing more queueing delays) comparing to the proposed algorithm with $V = V_1 = 1 \times 10^{-23}$.

In Figures 3(b), 3(d), and 3(f), energy consumption behaviors with strategic stochastic control are simulated and plotted with various V values. As presented in Figures 3(b), 3(d), and 3(f), more queue stability takes more energy consumption (especially refer to Figures 3(c) and 3(d)). This is reasonable due to the fact that more energy consumption for more transmit power allocation definitely leads to the stability of queues due to the fact that it will process more bits from the queue via increased SNR. The average energy consumption values and queue stability points with various three V settings are presented in Table 2.

As shown in Table 2, the tradeoff between energy-efficiency and queue stability is observed with various V settings. In this case, due to the fact that energy-efficiency and queue stabilization have tradeoff relationship, more queue

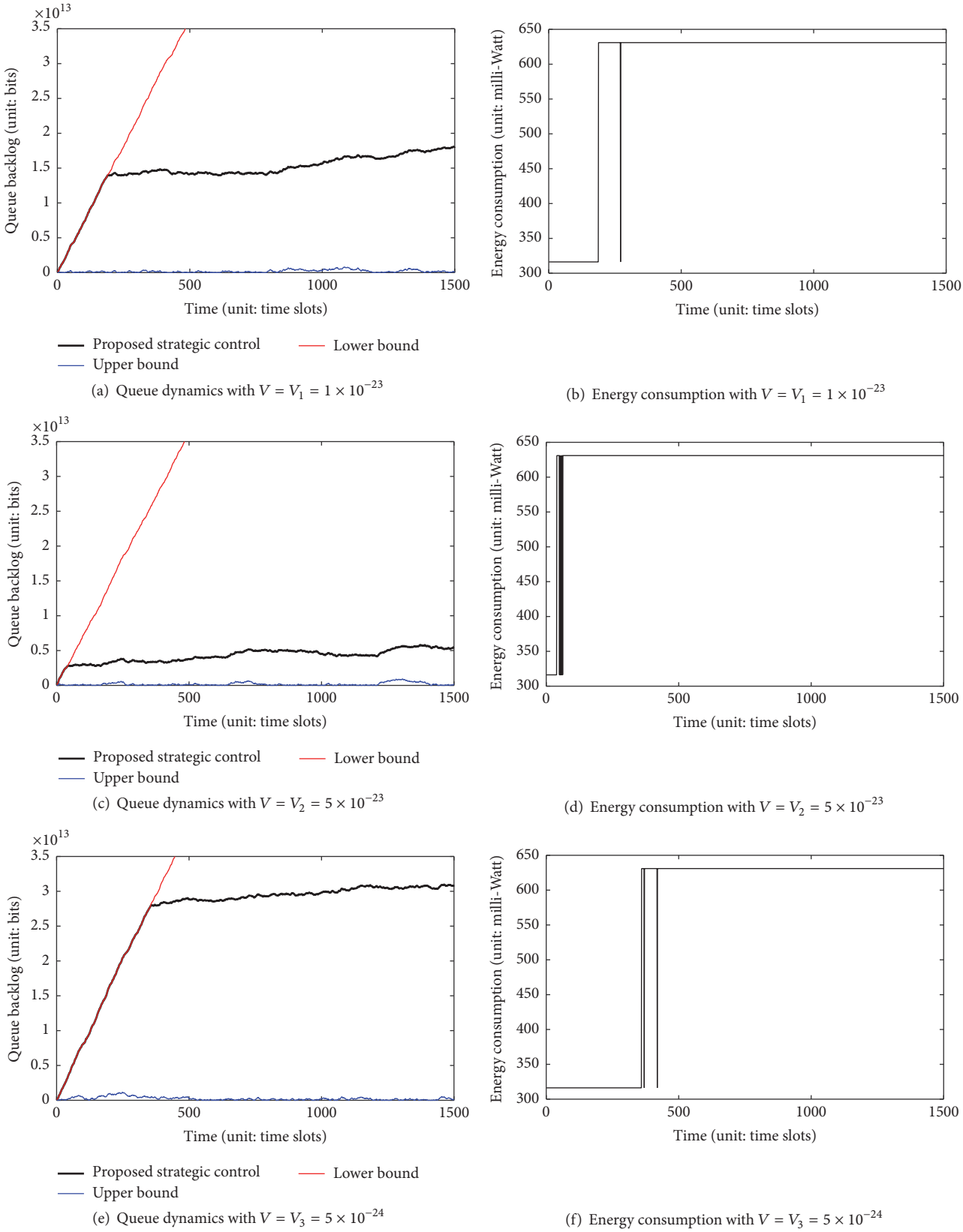

(a) Queue dynamics with $V = V_1 = 1 \times 10^{-23}$

(b) Energy consumption with $V = V_1 = 1 \times 10^{-23}$

(c) Queue dynamics with $V = V_2 = 5 \times 10^{-23}$

(d) Energy consumption with $V = V_2 = 5 \times 10^{-23}$

(e) Queue dynamics with $V = V_3 = 5 \times 10^{-24}$

(f) Energy consumption with $V = V_3 = 5 \times 10^{-24}$

FIGURE 3: Queue dynamics and energy consumption behaviors for our proposed stochastic algorithm with various V settings.

Table 2: Average energy consumption and queue stability point in each time slot with various V settings.

V	V_1	V_2	V_3
Energy consumption (unit: milli-Watt)	588.9934	623.8235	550.3866
Queue stability point (unit: bits)	$\approx 1.5 \times 10^{13}$	$\approx 0.5 \times 10^{13}$	$\approx 3 \times 10^{13}$

stabilization takes more energy. Therefore, the proposed algorithm with $V = V_2 = 5 \times 10^{-23}$ is less energy-efficient. This result states that the proposed algorithm with $V = V_2 = 5 \times 10^{-23}$ is more suitable for real-time (or time critical) VR video contents. However, this (setting V as big as possible) definitely introduces more energy consumption; that is, setting V as big as possible is not always good. In this case, the system needs to consider additional energy provisioning mechanisms (e.g., more lithium battery allocation and self-charging mechanism investigation in hardware platforms).

Notice that our considering stochastic network optimization and control theory formulated in (24) shows that higher V value setting provides more weights on queue stabilization. This theoretical discussion is verified with this simulation result.

6. Concluding Remarks and Future Work

This paper proposes a strategic stochastic control algorithm that is for the minimization of time-average expected power consumption subject to queue stability in distributed VR network platforms. In distributed VR network platforms, the VRS contains VR contents that should be transmitted to the head-mounted VRD. For the wireless transmission, 60 GHz mmWave wireless communication technologies are used owing to their high-speed massive data transmission (i.e., multi-Gbps data speed). On top of this 60 GHz wireless link from VRS to its associated VRD, a stochastic queue-stable control algorithm is proposed to minimize the time-average expected power consumption. The VRS calculates the amount of transmit power allocation for transmitting bits from VRS to its associated VRD. If the amount of transmit power allocation at VRS is quite high, more bits will be processed from the queue. This control eventually stabilizes the queues whereas power (or energy) management is not optimal. On the other hand, the small number of bits will be processed from the VRS queue if the amount of transmit power allocation is not enough. Then the VRS queue should be unstabilized, which should introduce the queue overflows in the VRS. Therefore, an energy-efficient stochastic transmit power control algorithm is necessary to transmit bits from the VRS queue under the design rationale of the joint optimization of *energy-efficiency* and *buffer stability*. Our simulation results demonstrate that our proposed control algorithm achieves desired performance.

As one of major future research directions, realistic and automatic V value setting strategies will be studied for the real implementation of the proposed stochastic control algorithm in wireless VR platforms. One of preliminary results in terms of adaptive V setting is presented in [21].

Conflicts of Interest

The authors declare that there are no conflicts of interest regarding the publication of this paper.

Acknowledgments

This work was supported by the National Research Foundation of Korea (NRF Korea) under Grant 2016R1C1B1015406 and ETRI grant funded by the Korean government (16ZS1210, NZV μ-Grain Architecture for Ultra-Low Energy Processor). The related contents were presented by Joongheon Kim at Electronics and Telecommunications Research Institute (ETRI), Daejeon, Korea, on November 2016, with the title "Stochastic Control of 60 GHz Links for Distributed Virtual Reality Network Platforms."

References

[1] F. Ozkan, "Introducing VR first: unlocking the door to a future in virtual reality," *IEEE Consumer Electronics Magazine*, vol. 5, no. 4, pp. 25–26, 2016.

[2] P. Lelyveld, "Virtual reality primer with an emphasis on camera-captured VR," *SMPTE Motion Imaging Journal*, vol. 124, no. 6, pp. 78–85, 2015.

[3] J. P. Schulze, "Advanced monitoring techniques for data centers using virtual reality," *SMPTE Motion Imaging Journal*, vol. 119, no. 5, pp. 43–46, 2010.

[4] S. Kuriakose and U. Lahiri, "Understanding the psychophysiological implications of interaction with a virtual reality-based system in adolescents with autism: a feasibility study," *IEEE Transactions on Neural Systems and Rehabilitation Engineering*, vol. 23, no. 4, pp. 665–675, 2015.

[5] J. Kim, Y. Tian, S. Mangold, and A. F. Molisch, "Joint scalable coding and routing for 60 GHz real-time live HD video streaming applications," *IEEE Transactions on Broadcasting*, vol. 59, no. 3, pp. 500–512, 2013.

[6] W. Roh, J.-Y. Seol, J. Park et al., "Millimeter-wave beamforming as an enabling technology for 5G cellular communications: theoretical feasibility and prototype results," *IEEE Communications Magazine*, vol. 52, no. 2, pp. 106–113, 2014.

[7] T. S. Rappaport, F. Gutierrez, E. Ben-Dor, J. N. Murdock, Y. Qiao, and J. I. Tamir, "Broadband millimeter-wave propagation measurements and models using adaptive-beam antennas for outdoor Urban cellular communications," *IEEE Transactions on Antennas and Propagation*, vol. 61, no. 4, pp. 1850–1859, 2013.

[8] T. S. Rappaport, J. N. Murdock, and F. Gutierrez, "State of the art in 60-GHz integrated circuits and systems for wireless communications," *Proceedings of the IEEE*, vol. 99, no. 8, pp. 1390–1436, 2011.

[9] K. Venugopal and R. W. Heath, "Millimeter wave networked wearables in dense indoor environments," *IEEE Access*, vol. 4, pp. 1205–1221, 2016.

[10] N. Chen, S. Sun, M. Kadoch, and B. Rong, "SDN controlled mmWave massive MIMO hybrid precoding for 5G heterogeneous mobile systems," *Mobile Information Systems*, vol. 2016, Article ID 9767065, 10 pages, 2016.

[11] H. Kim, M. Ahn, S. Hong, S. Lee, and S. Lee, "Wearable device control platform technology for network application development," *Mobile Information Systems*, vol. 2016, Article ID 3038515, 2016.

[12] J. Kim, S. Kwon, and G. Choi, "Performance of video streaming in infrastructure-to-vehicle telematic platforms with 60-GHz radiation and IEEE 802.11ad baseband," *IEEE Transactions on Vehicular Technology*, vol. 65, no. 12, pp. 10111–10115, 2016.

[13] Oculus GearVR, https://www3.oculus.com/en-us/gear-vr/.

[14] E. Cuervo and D. Chu, "Poster: mobile virtual reality for head-mounted displays with interactive streaming video and likelihood-based foveation," in *Proceedings of the ACM International Conference on Mobile Systems, Applications, and Services (MobiSys '16)*, Singapore, June 2016.

[15] Facebook, https://code.facebook.com/posts/194023157622878/gear-vr-to-get-dynamic-streaming-for-360-video/.

[16] P. Debevec, G. Downing, M. Bolas, H.-Y. Peng, and J. Urbach, "Spherical light field environment capture for virtual reality using a motorized pan/tilt head and offset camera," in *Proceedings of the International Conference on Computer Graphics and Interactive Techniques (SIGGRAPH '15)*, Los Angeles, Calif, USA, August 2015.

[17] J. Kim, L. Xian, R. Arefi, and A. S. Sadri, "60 GHz frequency sharing study between fixed service systems and small-cell systems with modular antenna arrays," in *Proceedings of the IEEE Global Communications Conference (GLOBECOM) Workshop on Millimeter-Wave Backhaul and Access: From Propagation to Prototyping (mmWave)*, San Diego, Calif, USA, December 2015.

[18] J. Kim and A. F. Molisch, "Fast millimeter-wave beam training with receive beamforming," *Journal of Communications and Networks*, vol. 16, no. 5, pp. 512–522, 2014.

[19] A. Maltsev, E. Perahia, R. Maslennikov, A. Lomayev, A. Khoryaev, and A. Sevastyanov, "Path Loss Model Development for TGad Channel Models," IEEE 802.11-09/0553r1, May 2009.

[20] A. F. Molisch, *Wireless Communications*, Wiley-IEEE, New York, NY, USA, 2011.

[21] J. Kim, "Energy-efficient dynamic packet downloading for medical IoT platforms," *IEEE Transactions on Industrial Informatics*, vol. 11, no. 6, pp. 1653–1659, 2015.